

Cognition and Behavior

Multivariate Analysis of Evoked Responses during the Rubber Hand Illusion Suggests a Temporal Parcellation into Manipulation and Illusion-Specific Correlates

Placido Sciortino and Christoph Kayser

<https://doi.org/10.1523/ENEURO.0355-21.2021>

Department for Cognitive Neuroscience, Faculty of Biology, Bielefeld University, Universitätsstr. 25, 33615 Bielefeld, Germany

Abstract

The neurophysiological processes reflecting body illusions such as the rubber hand remain debated. Previous studies investigating the neural responses evoked by the illusion-inducing stimulation have provided diverging reports as to when these responses reflect the illusory state of the artificial limb becoming embodied. One reason for these diverging reports may be that different studies contrasted different experimental conditions to isolate potential correlates of the illusion, but individual contrasts may reflect multiple facets of the adopted experimental paradigm and not just the illusory state. To resolve these controversies, we recorded EEG responses in human participants and combined multivariate (cross-)classification with multiple Illusion and non-Illusion conditions. These conditions were designed to probe for markers of the illusory state that generalize across the spatial arrangements of limbs or the specific nature of the control object (a rubber hand or participant's real hand), hence which are independent of the precise experimental conditions used as contrast for the illusion. Our results reveal a parcellation of evoked responses into a temporal sequence of events. Around 125 and 275 ms following stimulus onset, the neurophysiological signals reliably differentiate the illusory state from non-Illusion epochs. These results consolidate previous work by demonstrating multiple neurophysiological correlates of the rubber hand illusion and illustrate how multivariate approaches can help pinpointing those that are independent of the precise experimental configuration used to induce the illusion.

Key words: body consciousness; body ownership; EEG; rubber hand; rubber hand illusion; self-consciousness

Significance Statement

The neurophysiological signatures of body illusions such as the rubber hand remain debated. To reconcile the fragmented picture painted by previous work, we capitalized on a representation-centered approach to analyze human EEG recordings using multivariate classification and designed our study around two experimental Illusion conditions and multiple non-Illusion conditions that varied the relative hand position, or the nature of the control object. Our results show illusion-specific activations early after stimulus onset and during a prolonged time window, thereby consolidating the fragmented picture in the literature.

Introduction

The neurophysiological processes underlying multisensory body perception and the sense of body ownership are often studied using illusions such as the rubber hand

(Botvinick and Cohen, 1998; Blanke, 2012; Longo and Haggard, 2012; Riemer et al., 2019). There, participants watch an artificial hand being stimulated in synchrony with their own occluded hand, which results in the illusory

Received August 31, 2021; accepted December 13, 2021; First published January 3, 2022.

The authors declare no competing financial interests.

Author contributions: P.S. and C.K. designed research; P.S. performed research; P.S. and C.K. contributed unpublished reagents/analytic tools; P.S. and C.K. analyzed data; P.S. and C.K. wrote the paper.

experience of the rubber hand becoming embodied (Tsakiris and Haggard, 2005; Blanke, 2012). Despite many behavioral (Botvinick and Cohen, 1998; Tsakiris and Haggard, 2005; Longo and Haggard, 2012) and neuroimaging studies (Ehrsson et al., 2004, 2005; Petkova et al., 2011; Bekrater-Bodmann et al., 2012; Brozzoli et al., 2012; Gentile et al., 2013; Guterstam et al., 2013; Limanowski and Blankenburg, 2016) involving the rubber hand illusion the underlying electrophysiological correlates, such as studied using EEG, remain debated.

In fact, previous electrophysiological studies disagree on the relevant illusion-specific activations. For example, several studies have investigated the evoked potentials produced by the repetitive visuo-tactile stimulation and asked when and how these responses are affected by the illusory state, that is, the subjective state of the individuals when they experience the rubber hand as becoming part of their own body, an experience that is absent in the control conditions. Some studies reported illusion-correlates only at early (~50 ms) latencies relative to the stimulation events and advocated for a low-level origin in early somatosensory cortex (Zeller et al., 2015; Sakamoto and Ifuku, 2021). Support for such an origin also comes from studies on the general enhancement of somatosensory processing by multisensory inputs on the viewed body (Cardini et al., 2011, 2012). However, other studies advocated for illusion-correlates only at latencies of around 120–200 ms, possibly related to the detection of mismatching sensory signals in temporo-parietal cortex (Press et al., 2008), while a third group of studies emphasized illusion-related activity at even longer latencies of around 300–400 ms and suggested high-level cognitive processes as underlying sources (Peled et al., 2003; Rao and Kayser, 2017). This body of previous work also diverges on whether perceiving the illusion would enhance or attenuate evoked responses (Zeller et al., 2015), with some studies on related body illusions reporting no localized changes in evoked activity at all (Pyasik et al., 2021).

One reason for these diverging results may be the different experimental settings used to induce the illusion. For example, the illusion has been induced when the real hand is besides (Lloyd, 2007; Kammers et al., 2011; Bekrater-Bodmann et al., 2014; Riemer et al., 2015; Rao and Kayser, 2017) or below the rubber hand (Rohde et al., 2011; Preston, 2013; Zeller et al., 2015), resulting for example in possibly different illusion onset times. Another reason may be that few studies asked which neurophysiological signatures generalize across experimental settings used to isolate the neurophysiological correlates of the

illusory state. While individual studies reported correlates at different latencies, it remains unclear at which latencies (early, intermediate, or late) relative to the visuo-tactile stimulation brain activity reliably differentiates the illusory state from multiple and suitable control conditions. This question about neural representations generalizing across experimental contrasts, however, is difficult to address in the classical activation-mapping framework used by previous studies, for two reasons (Kriegeskorte et al., 2006; Hebart and Baker, 2018). First, the analysis of electrode-wise evoked responses implicitly assumes a common reference model of the brain and the same spatial configuration of the relevant illusion-related activations across participants. Yet, the individual variability in brain morphology may invalidate this assumption (Van Horn et al., 2008; Li et al., 2019; Eichert et al., 2020) and one study on bodily illusions provided direct evidence that illusion-specific correlates have been reflected in distributed rather than localized patterns of EEG responses (Aspell et al., 2012). Second, the typical pairwise comparison of experimental conditions makes it difficult to generalize significant differences across multiple experimental conditions, a critical test required to establish which neurophysiological signatures generalize across experimental settings used to induce the illusion (Kriegeskorte et al., 2006; Hebart and Baker, 2018).

In an attempt to address this challenge, the present study employed a linear multivariate classification framework to probe whether and when neurophysiological correlates of the illusory state generalize across distinct illusion-inducing configurations. Such a linear classification framework has been ubiquitously used to uncover the neurophysiological representations of sensory and cognitive processes (Parra et al., 2005; Cichy et al., 2014; Grootswagers et al., 2018; Guggenmos et al., 2018; Keitel et al., 2020), and, rather than constraining the relevant sources in space to be identical across participants, it allows relying on the statistical properties of the data (Parra et al., 2005; Blankertz et al., 2011; Grootswagers et al., 2017, 2018). We here exploit this approach to overcome the two above mentioned problems: it allows us to directly probe whether and when neurophysiological correlates of the illusory state generalize across distinct illusion-inducing configurations, and it allows for distinct spatial patterns of neurophysiological illusion correlates in individual participants.

To this end, we combined EEG recordings in human participants with a computer-controlled setup to induce the illusion, allowing the precise alignment of rapid neurophysiological responses to the experimental stimulation (Rao and Kayser, 2017). Importantly, to address the question of when neurophysiological signatures generalize across experimental conditions, we employed two experimental configurations to induce the illusion (having the rubber hand besides or below the participant's hand), two non-illusion control conditions (a body-incongruent rubber hand tilted by 90°, and participant's real hand), and we investigated a contrast devoted to comparing evoked responses within the same experimental illusion trial, between the period before and after participants reporting the onset of the illusion, a contrast already explored in

C.K. was supported by the European Research Council (ERC-2014-CoG) Grant 646657.

Acknowledgements: We thank Alexander Wecker for help with implementing the experimental setup.

Correspondence should be addressed to Placido Sciortino at placido.sciortino@uni-bielefeld.de.

<https://doi.org/10.1523/ENEURO.0355-21.2021>

Copyright © 2022 Sciortino and Kayser

This is an open-access article distributed under the terms of the [Creative Commons Attribution 4.0 International license](https://creativecommons.org/licenses/by/4.0/), which permits unrestricted use, distribution and reproduction in any medium provided that the original work is properly attributed.

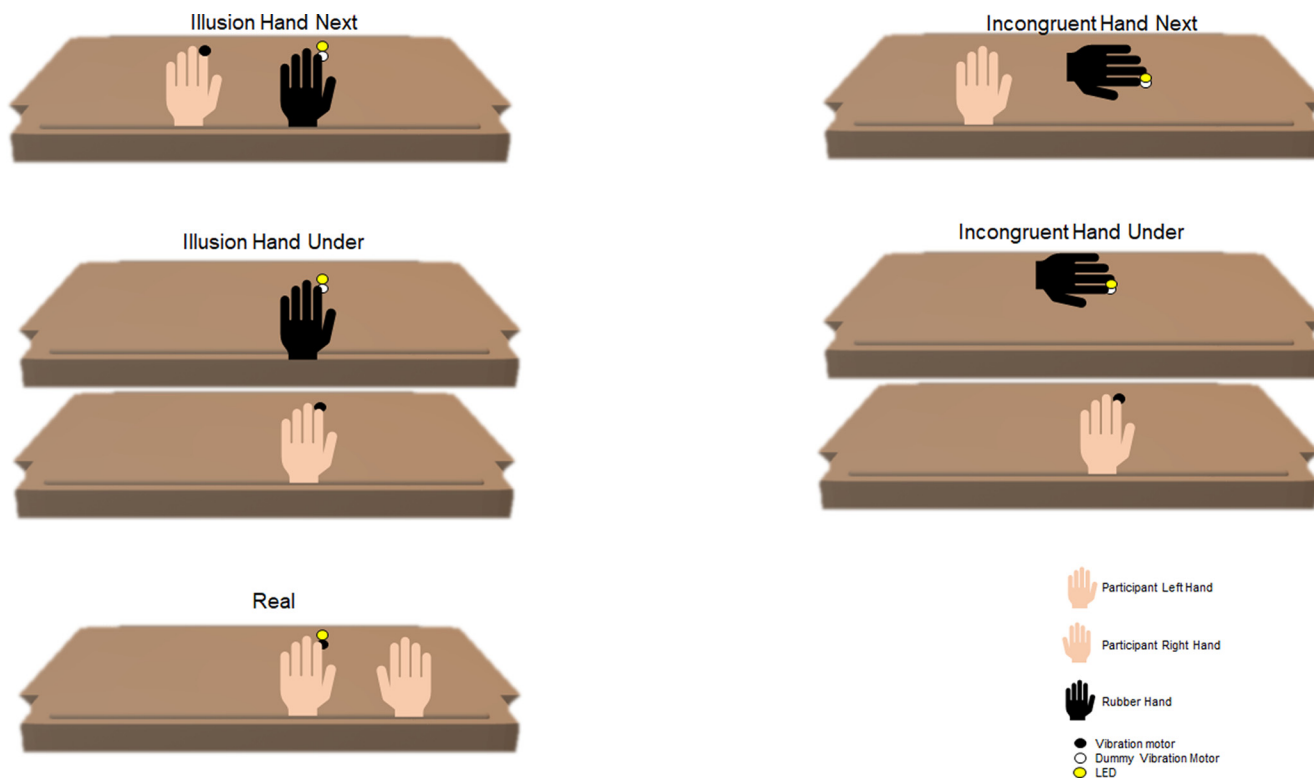


Figure 1. Schematic of the five experimental conditions. The experiment involved two Illusion conditions that differed in the spatial arrangement of the real and artificial limbs (horizontal or vertical displacements), and the two respective Incongruent conditions obtained by rotating the rubber hand into an unphysiological body position by 90°. Finally, we included a Real condition in which the rubber hand was absent and multisensory stimulation was delivered to the participant's real hand.

fMRI and EcoG studies (Ehrsson et al., 2004; Guterstam et al., 2019). We complemented the EEG recordings with measurements of skin conductance, an index of autonomous responses that is sensitive to the embodiment of a rubber hand (Armell and Ramachandran, 2003; Ehrsson et al., 2007; Gentile et al., 2013; D'Alonzo et al., 2020). This allowed us to ask the more explorative question of whether the neurophysiological correlates of the illusory state are related to these bodily correlates.

In sum, by employing a multivariate framework our study aimed to make methodological advances on how the neurophysiological signatures of body illusions can be investigated. Our results provide conceptually novel results by highlighting when in time neurophysiological signatures possibly generalize across experimental conditions, and help to reconcile the diversity of results reported in previous EEG studies on the rubber hand illusion (also abbreviated in RHI from now on).

Materials and Methods

Experimental conditions

Experiments were performed in a darkened and electrically shielded room (Ebox, Desone). Participants sat on a comfortable chair in front of a one-compartment, open-ended box placed on a two-story wooden platform. Five experimental conditions were used (Fig. 1). These differed in the relative position of participant's hand relative to the rubber hand (besides or below the rubber hand hand), the

relative orientation of the rubber hand (rubber hand aligned to the body, or tilted by 90°), or did not involve any rubber hand (with the stimulation on the real hand). Each trial lasted 3 min and consisted of 180 visuo-tactile stimulation events of 100-ms duration and presented with an interstimulus interval (ISI) was 900 ms, resulting in a visuo-tactile stimulation frequency of 1 Hz. Visual stimuli were delivered by white light-emitting diodes (LED; Seeedstudio, 10-mm diameter) and tactile stimuli were delivered to the participant's fingertip by a vibration motor (Grove: Vibration motor, Seeedstudio). Both stimuli were controlled via MATLAB and two Arduino Uno prototyping platforms. To facilitate the alignment of stimulation events with the EEG data we routed a copy of the voltage controlling the DC motor to an analog input of the EEG system.

The precise experimental conditions were designed as follows. In the Illusion Hand Next condition, a lifelike rubber hand (for men: a silicon cosmetic glove, model 102LS, for women: model 102LS, ORTHO-REHA Neuhof GmbH) was positioned on top of the platform (horizontal plane) in front of the participants in an anatomically congruent orientation, as typically used to induce the illusion. The index finger of the rubber hand was placed on a dummy vibration motor, which did not vibrate. The participant's left hand was covered with a blanket, hidden to the participant's view, and was positioned at a distance of 10 cm

Table 1: Questionnaire used to assess the subjective feeling of the illusion (adapted from Botvinick and Cohen, 1998)

1	During the last trial it seemed as I were feeling the touch in the location where I saw the rubber hand touched	Illusion
2	During the last trial it seemed as though the touch I felt was caused by the vibration motor under the rubber hand	Illusion
3	During the last trial I felt as if the rubber hand were my hand	Illusion
4	During the last trial it felt as my (real) hand was drifting towards the rubber hand	Control
5	During the last trial it seemed as I might have more than one left hand or arm	Control
6	During the last trial it seemed as if the touch I was feeling came from somewhere between my own hand and the rubber hand	Control
7	During the last trial I felt as my (real) hand was turning rubbery	Control
8	During the trial it appeared (visually) as if the rubber hand were drifting towards left (towards my hand)	Control
9	During the trial the rubber hand began to resemble to my own hand in term of shape, skin tones, freckles or some other features	Control

The questionnaire included nine statements describing the underlined phenomena. Participants indicated their response on a 7-scale ranging from “strongly agree” (−3) to “strongly disagree” (+3).

from the rubber hand in the horizontal plane. The tip of the participant’s index finger was placed on the vibration motor, while the right hand was placed at the other end of the platform in reaching distance of a keyboard. The LED was positioned 5 mm above the dummy motor near the rubber hand. The somatosensory stimulus on the participant’s hand and the synchronous visual stimulus near the rubber hand reliably induce the illusion, as discussed below. In the Incongruent Hand Next condition, the rubber hand was placed in an anatomically incongruent position at a 90° angle. In the Illusion Hand Under condition, the rubber hand was placed in front of the participant, while the participant’s real hand was covered with a blanket and placed in the lower panel of the platform 10 cm under the rubber hand in the vertical plane. Otherwise, the setup was the same as for the Illusion Hand Next condition. In the Incongruent Hand Under condition, the rubber hand was placed in an anatomically incongruent position, at a 90° angle below participants’ hand. We also included a control condition in which the rubber hand was absent. In this Real condition, no rubber hand was present, and the index finger of the left hand was placed on a vibration motor positioned 5 mm below the LED. The right hand was in the same position as in the Illusion and Incongruent conditions. In the following text, we denote with the capitalized Illusion, the respective experimental conditions, while we use the non-capitalized Illusion to refer to the phenomenon in general.

The five experimental conditions were presented in a pseudorandomized order for each participant. Each condition was repeated four times, for a total of 20 trials per participant. The choice of a rotated rubber hand for the Incongruent condition was made based on previous studies showing that an unrealistic posture abolishes the illusion reliably (Pavani et al., 2000; Ehrsson et al., 2004; Rao and Kayser, 2017; Riemer et al., 2019). Importantly, another often used control condition involving the asynchronous stimulation of the real and rubber hands can result in participants also reporting the illusion in presumed control conditions, and makes specific assumptions about the temporal duration of the multisensory binding window, which the Incongruent condition avoids (Valenzuela Moguillansky et al., 2013; Costantini et al., 2016; Fuchs et al., 2016). The Real condition involves the stimulation of the participant’s real hand, while maintaining the same posture and position of the rubber hand, varying only the

nature of the embodied limb (rubber hand in the Illusion condition, real hand in the Real condition; Zeller et al., 2015, 2016; Rao and Kayser, 2017). Since the posture and the nature of the stimulation was the same as for the Illusion condition, we hypothesized that any change between the Illusion and the Real should reflect the illusory feeling and the nature of the embodied object, a dimension not probed by the misalignment of any real and artificial hands or by the asynchronous stimulation of the artificial hands as has been used in some previous studies.

We chose a computer-controlled stimulation setup using LED stimuli as a previous study has shown that such a setup can reliably induce the RHI (Rao and Kayser, 2017). In particular, the LED and vibration stimulus provide a synchronized reference frame between the participant’s real hand and the rubber hand, which leads to the induction of the illusion (Shimada et al., 2009; Evans and Blanke, 2013; Bekrater-Bodmann et al., 2014; Rao and Kayser, 2017). Indeed, previous work has shown that the RHI can be reliably induced across different setups and manipulations that do not necessarily need to involve the presence of an experimenter stroking both hands with a brush (Bertamini and O’Sullivan, 2014; Kalckert and Ehrsson, 2014; Guterstam et al., 2015; Rao and Kayser, 2017). Furthermore, the brief and temporally precise stimulation provided by LED and the vibration motor allows the precise alignment of rapid neurophysiological signals to the stimulation sequence, which becomes intrinsically difficult with temporally imprecise events such as manual stroking (Rao and Kayser, 2017).

Participants

To ensure that participants enrolled in the main EEG experiment were indeed able to feel the illusion, we conducted a pretest on participants of either sex. None of the participants tested in the pretest reported having participated in a study involving the rubber hand or similar body illusions before. During the pretest four conditions were presented in pseudo-random order (the two Illusion conditions and their respective Incongruent conditions), each presented once. To probe whether or when participants felt the illusion, we capitalized on question three from the common rubber-hand questionnaire (Table 1; Botvinick and Cohen, 1998). Specifically, we instructed participants

to press (using their right hand) a key on a computer keyboard when they were “feeling the rubber hand as belonging to their body.” After each trial, they were asked to also verbally confirm that this statement applied. For the main study we invited only participants who in the pretest had indicated feeling the illusion in both Illusion conditions and who did not report feeling the illusion in any Incongruent condition. The criteria to be included in the main study were reporting the illusion onset with a button press, a mean positive score for the three illusion statements and a mean negative score for the control statements (Botvinick and Cohen, 1998). A total number of 24 healthy right-handed participants (9 males, 15 females) participated in this study were included in the main study. That only about half the pretested naive participants reported feeling the illusion in the present experiment is largely in line with previous work, where reported numbers vary between half and two-thirds (Ehrsson et al., 2004, 2007; Lloyd, 2007; Rao and Kayser, 2017; Riemer et al., 2019; Reader et al., 2021, p 202). All participants gave written informed consent before participation in accordance with the Declaration of Helsinki. All protocols conducted in this study were approved by the Ethics Committee of Author University.

The main experiment took place on a different day than the pretest. During the main experiment four repeats of each of the five conditions were administered in pseudo-random order for each participant, hence comprising 20 trials in total. Each condition lasted for 3 min of visuo-tactile stimulation (180 stimulation events). Because administering the rubber hand questionnaire 20 times is unlikely to yield sensitive results, we capitalized on the button press response as a practical and brief implementation of a test of the main item of the questionnaire, i.e., question three on the embodiment of the rubber hand. We hence relied on this as an index of whether and when during each trial participants started to feel the illusion. We also administered the full questionnaire (Table 1; Botvinick and Cohen, 1998) at the end of the first repeat of each of the two Illusion conditions. From these we calculated the average scores for illusion (Illusion Hand Next: 2.38 ± 0.53 , mean \pm SEM; Illusion hand under: 2.61 ± 0.53) and control statements (hand next: -1.47 ± 0.76 ; hand under: -1.56 ± 0.80), which suggest that participants were indeed feeling the illusion. One participant was excluded from the main study as this participant reported feeling the illusion also during one Incongruent trial and one participant was excluded because of reporting the illusion for only one of the two Illusion conditions. Hence, we report EEG data for an n of 22.

EEG recording and preprocessing

EEG signals were continuously recorded using a 128 channel BioSemi (BioSemi, B.V.) system with Ag-AgCl electrodes mounted on an elastic cap (BioSemi). Four additional electrodes were placed at the outer canthi and below the eyes to obtain the electro-oculogram (EOG). Electrode offsets were kept below 25 mV. Data were acquired at a sampling rate of 1028 Hz. Data analysis was performed with MATLAB (The MathWorks Inc.) using the FieldTrip toolbox (Oostenveld et al., 2011). Data were

bandpass filtered between 0.6 and 90 Hz, and resampled to 200 Hz as in our previous work (Kayser and Kayser, 2020; Park and Kayser, 2021) for further processing. Subsequently, the data were denoised using Independent component analysis (ICA) and components reflecting muscular artefacts, eye blinks, eye movements as well as poor electrode contacts were identified based on recommendations in the literature and confirmed based on visual inspection (O’Beirne and Patuzzi, 1999; Campos Viola et al., 2009; Hipp and Siegel, 2013). Overall, we removed an average of 15.0 ± 1 (mean \pm SEM) components per participant, a number comparable to previous studies using a very similar analysis pipeline (Grabot and Kayser, 2020; Bröhl and Kayser, 2021; Park and Kayser, 2021).

For subsequent data analysis, we epoched the data around each visuo-tactile stimulation event, with epochs lasting from -400 ms prestimulus to 400 ms poststimulus onset. This resulted in a total number of 180 epochs for each trial. Epochs were combined within each condition, were bandpass filtered between 1 and 40 Hz (two-pass third order Butterworth filters) using the FieldTrip toolbox, to emphasize within-epoch changes and to remove slow drifts that span multiple epochs (Park and Kayser, 2021). Epochs with signals exceeding a level of $165 \mu\text{V}$ were considered as artifact and removed. Importantly, to render the main analysis of the Illusion conditions specific to participants experiencing the illusory state, we only included epochs after the time point at which participants indicated the onset of the illusion. Hence for any analysis of the Illusion conditions, we included only epochs after the trial-specific onset of the subjective illusion state. Because this effectively removes the early epochs in each 3-min trial, we applied a similar selection to the other conditions; here, we removed epochs before the participant-specific median reaction time obtained from all Illusion trials. The resulting number of epochs available for each condition for both Illusion conditions was 897 ± 51 (mean \pm SEM), for the Incongruent conditions 845 ± 56 , and for the Real condition 434 ± 33 epochs. In a separate analysis, we contrasted the epochs of the Illusion trials before the illusion onset with those in the Illusion trials subsequent to the illusion onset.

Analysis of EEG activity using single-trial classification

To quantify whether and when EEG activity differed between experimental conditions, we used single-trial classification based on a regularized linear discriminant analysis (LDA; Parra et al., 2005; Blankertz et al., 2011). We used this specific classifier as it has been successfully used over the last decade in conjunction with neuroimaging data and because it has proven equally powerful as computationally more complex algorithms (Grootswagers et al., 2017). As typical for LDA analyses, the epoched data were binned into overlapping time bins: we here relied on bins of 60-ms duration, and the classifier was computed at 10-ms time steps, similar as in our previous work (Park and Kayser, 2021). The analysis thereby emphasizes the low-frequency components of the recorded EEG signals, which have highest signal-to-noise ratio and are less contaminated by muscular or ocular artefacts, in contrast to high frequency activity (Hipp and Siegel,

Table 2: Classification results

	<i>p</i> -value	AUC_sum	Time interval	Max AUC	Time of max AUC (s)
Illusion vs Incongruent	<0.001	3.68	[0.065–0.325]	0.68	0.125
Illusion vs Real	<0.001	3.90	[0.075–0.305]	0.70	0.135
Illusion vs Incon. “next”	<0.001	3.88	[0.07–0.305]	0.70	0.125
Illusion vs Incon. “under”	<0.001	2.97	[0.08–0.305]	0.67	0.135
Within Illusion trials	<0.001	3.43	[0.03–0.300]	0.65	0.13
Cross: (Ill vs Incon.) to (Ill vs Real)	=0.001	0.33	[0.075–0.155]	0.54	0.125
	0.011	0.19	[0.265–0.315]	0.53	0.275
Cross: (Ill vs Incon. “next”) to (Ill vs Incon. “under”)	0.002	0.32	[0.45–0.125]	0.54	0.095
	<0.001	0.48	[0.155–0.265]	0.56	0.185
Cross: (Ill vs Incon.) to (Within Illusion trials)	-	-	-	0.52	0.30

The table lists all pairwise classification and cross-classification (Cross:) results reported in the study. For each classifier we report the *p*-value of the significant cluster(s), the cluster statistics (AUC_sum), the time interval of the significant cluster(s), the maximal AUC value, and the time point of this.

2013). The data are shown such that the time axis refers to the center of these 60-ms time bins. The regularization parameter was set to 0.1 as in previous work (Park and Kayser, 2019), and we based the classifier on “pseudo-trials” obtained from four epochs. For each participant, the classifier performance was obtained as the receiver operating characteristic area under curve (AUC), computed from sixfold cross-validation (preliminary tests had revealed that using more cross-validation folds provides no benefit to the results). That is, we trained the data on five-sixth of the data and tested the classification performance on the remaining one-sixth of the data. Because the available epoch numbers differed across conditions, we relied on a re-sampling procedure: classification performance was derived by randomly selecting equal numbers of epochs for each contrast (randomly selecting a number of trials that corresponds to 80% of the smaller number of available epochs for each condition, and averaging the classification performance over 50 repeats of this procedure). We derived participant-wise scalp topographies for each classifier by estimating the corresponding forward model, defined as the normalized correlation between the discriminant component and the EEG activity (Parra et al., 2005). The group-averaged forward models at time points of interest are shown as insets in Figures 4, 5.

Importantly, by combining the signals from all electrodes into the multivariate classification process, this analysis does not make the assumption that the condition-wise spatial configuration of the relevant activity is the same across participants. Rather, it allows experimental conditions to differ reliably within each participant by a specific spatial pattern of activity, but this pattern can differ between participants. The analysis implemented here effectively asks whether at any moment during the data epoch one can reliably differentiate two conditions in each individual participant such that the group-level classification performance is significantly different from chance, see below for the statistical details (Cichy and Teng, 2017; Grootswagers et al., 2017). This classification analysis was used to test for EEG responses differentiating: (1) the Illusion versus Incongruent epochs (across both hand positions, Fig. 4A; and separately for each hand position, Fig. 4B); (2) the Illusion versus Real epochs (Fig. 4A); (3) and for activity differentiating those epochs within the Illusion trial before the onset of the illusory state (hence

before participant’s button press) versus those during the illusion (i.e., after the button press; Fig. 5A).

To directly test whether the neurophysiological signatures discriminating the Illusion and Incongruent conditions are the same as those also differentiating the Illusion and Real conditions, we used cross-classification (Kaplan et al., 2015). For this, we trained the classifier on half the Illusion and half the Incongruent trials and then applied classifier weights to differentiate the remaining half of the Illusion and Real trials, repeating this procedure 50 times. Cross-classification was quantified using the AUC and computed for both directions: training on Illusion versus Incongruent and testing on Illusion versus Real, and training on Illusion versus Real and testing on Illusion versus Incongruent. The respective AUC values for each participant and time point were averaged over both directions and repeats of the calculation (Fig. 4C). The same cross-classification analysis was also used to test whether the neurophysiological signatures discriminating Illusion and Incongruent for the “hand next” arrangement generalize to the “hand under” arrangement (Fig. 4D), and to test whether classifiers trained on the discrimination of Illusion versus Incongruent also generalize to the discrimination of the epochs before the Illusion versus those during the Illusion (reported in text). A summary of all classification results is also provided in Table 2.

Recording of skin conductance signals

Skin conductance was continuously recorded using a Neulog GSR logger NUL-217 sensor with Ag/AgCl electrodes were placed on the palmar sites of the middle and ring finger of the participant’s left hand. GSR measurements were recorded in micro-Siemens and at a sampling rate of 100 Hz. For offline analysis the data were resampled to 50 Hz, bandpass filtered between 0.5 and 2 Hz (third-order Butterworth filter). Trials were visually inspected and few trials with artefacts were manually removed. For a few participants ($n=2$) the skin conductance data were incomplete, as the software had crashed during recording. Hence the effective participant sample for EEG ($n=22$) and skin responses ($n=20$) differed.

Analysis of skin conductance data

We opted for an analysis that directly contrasts the skin conductance in two adjacent time windows of 3-s

duration. These windows were chosen around the key event of interest: the trial-specific onset of the illusion indicated by participants pressing the response button. The duration of the analysis window was chosen as a compromise between the typical latency of changes in skin conductance after an event (Boucsein et al., 2012; Sjouwerman and Lonsdorf, 2019) and the reaction times at which participants started feeling the illusions. To quantify the change in skin conductance (termed “skin response”) induced by the illusion onset we computed the standard deviation of the signal in two adjacent windows around the illusion onset (e.g., $[-3, 0]$ s and $[0, +3]$ s with 0 being the illusion onset time) and computed their ratio. In one analysis we computed the ratio between the window immediately following the illusion onset ($[0, +3]$ s) and the immediately preceding window ($[-3, 0]$ s). In a second analysis, we focused on the ratio of the two windows immediately before the illusion onset (hence $[-3, 0]$ s and $[-6, -3]$ s). To calculate the standard deviation (and then, their ratio) for Incongruent and Real conditions, we used trial-number-specific reaction times obtained from the Illusion trial with that respective number as surrogate time points to define the corresponding windows.

Statistics

Statistical testing of the classification performance (AUC values) relied on a randomization approach and cluster-based permutation procedures to control for multiple comparisons (Nichols and Holmes, 2002; Maris and Oostenveld, 2007). Following recommendations in the literature we implemented a group-level random-effects inference on the null hypothesis of no experimental effect, which here corresponds to classification performance being around chance (Cichy and Teng, 2017; Grootswagers et al., 2017). In general, this is obtained by permuting the participant-wise condition labels of the test of interest (Maris and Oostenveld, 2007). Here, the randomization distribution was obtained by shuffling the sign of the true single-participant effects (i.e., the sign of the chance-level corrected AUC values) based on which we derived a distribution of expected group-level effect of no systematic classification performance across participants. We relied on 5000 randomizations for each test, used a cluster-forming threshold corresponding $p < 0.01$ (i.e., using the 99th percentile of the full distribution of randomized AUC values), applied spatial clustering based on a minimal cluster size of 3, and used the sum of AUC values within each cluster as cluster-wise test statistics. For significant clusters we report the cluster statistics (summed AUC value) and the peak classification performance (max AUC). The correlation between classification performance and differences in skin responses between Illusion and Incongruent conditions was based on a between-participant Pearson correlation, and statistical significance was established again using a cluster-based permutation approach, using a first-level threshold of $p < 0.01$ and by shuffling the assignment of AUC values and skin responses across participants. To compare the median latencies of illusion onsets between conditions and to compare the skin responses between pairs of conditions we used Wilcoxon signed-rank tests.

Effect sizes for this test were obtained using the point-biserial correlation (denoted r_{rb} ; Kerby, 2014).

Results

Illusion onset times

We compared the mean onset times of the illusory states between the two Illusion conditions. The onsets in the “hand next” condition occurred on average after 51 ± 7.7 s ($n = 22$; mean \pm SD; median: 42 s) and significantly later compared with the “hand under” condition (34 ± 5.9 s, mean \pm SD; median: 30 s; Wilcoxon signed-rank test $Z = 2.13$, $p = 0.03$, $r_{rb} = 0.45$). Hence, the hand under arrangement required less time to induce the illusion, despite the physical distance between the participant’s and the rubber hand being the same in both configurations. We note that these latencies are comparable to previous work using a similar experimental setup (Rao and Kayser, 2017).

Skin conductance

We implemented two explorative analyses focusing on changes in skin conductance emerging either in parallel with the participant’s overt response of feeling the illusion (button press), or before this. The analysis centered on the reported illusion onset revealed no significant differences in skin response between Illusion and Incongruent conditions ($n = 20$, Wilcoxon sign-rank test, $Z = -2.13$, $p_{corr} = 0.100$, $r_{rb} = -0.54$; Fig. 2, left) or between Illusion and Real conditions ($Z = -0.6$, $p_{corr} = 0.82$, $r_{rb} = -0.15$, with p -values corrected across tests using the Benjamini–Hochberg procedure). The analysis focusing on the epochs before the onset revealed significantly stronger skin responses during the Illusion compared with the Incongruent condition ($Z = 2.99$, $p_{corr} = 0.003$, $r_{rb} = 0.76$; Fig. 2, right), but not between the Illusion and Real conditions ($Z = 0.26$, $p_{corr} = 0.79$, $r_{rb} = -0.06$).

Evoked responses differ between Illusion and control conditions at multiple latencies

We then asked whether and how EEG activity differs between epochs in which participants feel the illusion (i.e., the illusory state) and the different non-Illusion conditions. Specifically, we focused on the electrophysiological responses evoked by the repetitive visuo-tactile stimulus as a signature of the cerebral processing of the repetitive visuo-tactile stimuli used to induce the illusion. To illustrate these, Figure 3 shows the trial-averaged and participant-averaged evoked responses. This suggests that differences between the three main experimental conditions may exist at various points in time and for a prolonged time.

To systematically probe for differences in the spatio-temporal patterns of evoked responses between conditions, we relied on a multivariate classification framework. Group-level classification performance of Illusion versus Incongruent epochs was significant from 0.065 to 0.325 s ($n = 22$, cluster-based permutation test correcting for multiple comparisons along time, $p < 0.001$, AUC_{sum} = 3.68, max AUC = 0.68 at 0.125 s; Fig. 4A; see also Table 2

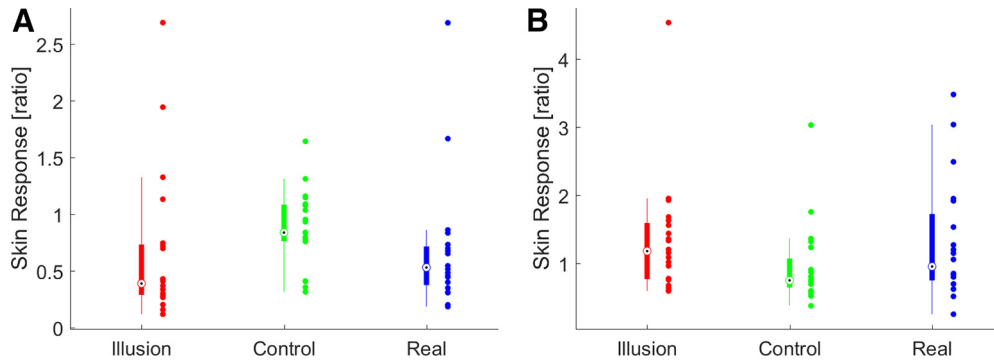


Figure 2. Changes in skin conductance associated with the illusion. Boxplots show skin responses for the two time windows: **(A)** around the illusion onset ($[-3, 0\text{ s}]$ to $[-0, +3\text{ s}]$) and **(B)** before the reported onset of the illusion ($[-6, -3\text{ s}]$ to $[-3, 0\text{ s}]$). Skin responses were defined as the ratio of the conductance in the two windows of interest. Boxplots indicate the median (circle) and 25th and 75th percentiles (thick line). Dots indicate individual participants ($n = 20$).

for an overview over all classification results). In a subsequent analysis we confirmed that the difference between Illusion and Incongruent conditions prevailed for both relative positions of the artificial and real hands: classification of each Illusion versus the respective Incongruent condition was significant in similar time windows (“hand next”: from 0.075 to 0.305 s, $p < 0.001$, $AUC_{sum} = 3.88$, max $AUC = 0.70$ at 0.125 s; “hand under”: from 0.08 to 0.305 s, $p < 0.001$, $AUC_{sum} = 2.97$, max $AUC = 0.67$ at 0.135 s; Fig. 4B). Classification of the Illusion versus the Real condition was significant in a similar long window (cluster from 0.075 to 0.305 s, $p < 0.001$, $AUC_{sum} = 3.90$, max $AUC = 0.70$ at 0.135 s; Fig. 4A).

We then asked whether the representational differences between the Illusion and Incongruent conditions and between Illusion and Real conditions arise from the

same neurophysiological processes and hence have a similar spatial configuration within each participant. To address this question we relied on the concept of cross-classification (Kaplan et al., 2015; Cichy and Teng, 2017). Practically, this was implemented by training the classifier to discriminate between one pair of conditions (e.g., Illusion vs Incongruent) and testing this on another pair (e.g., Illusion vs Real) using non-overlapping sets of trials. The cross-classification performance was significant in two clusters (between 0.075 and 0.155 s, $p = 0.001$, $AUC_{sum} = 0.33$, max $AUC = 0.54$ at 0.125 s; and between 0.265 and 0.315 s, $p = 0.011$, $AUC_{sum} = 0.19$, max $AUC = 0.53$ at 0.275 s; Fig. 4C), suggesting that during these times the Illusion epochs are distinguished from both types of non-Illusion epochs by a consistent pattern of evoked response. We also used cross-

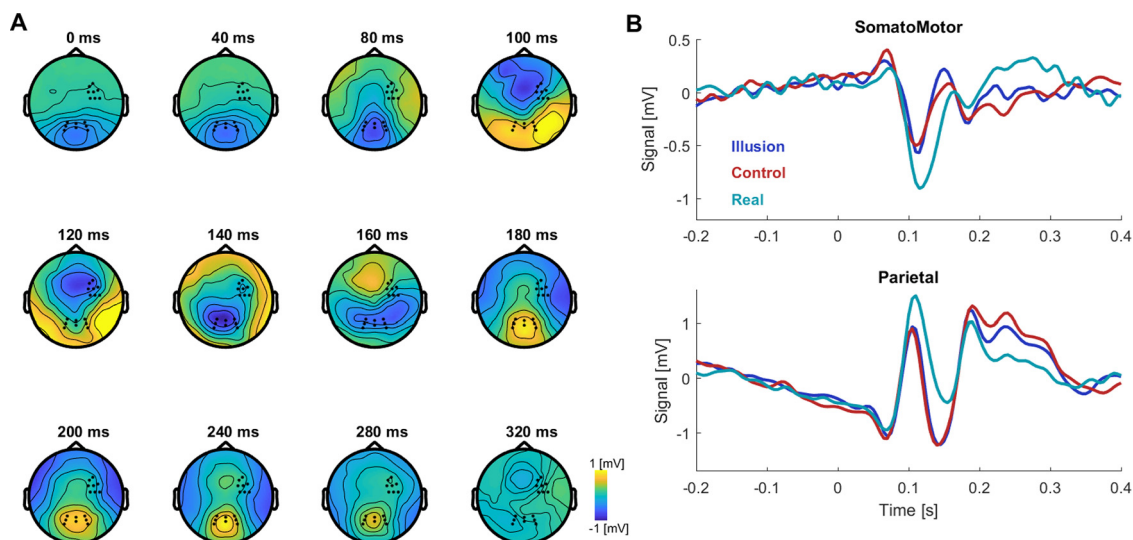


Figure 3. Illustration of evoked responses. **A**, Average response across all experimental conditions shown as topographical time course aligned on the onset of the repetitive visuo-tactile stimuli at time 0 ($n = 22$). **B**, Time courses for two regions of interest (the respective electrodes are indicated in the topographies in panel **A**). Regions of interest were defined over right somato/motor electrodes based on their position in the EEG BioSemi cap and on previous studies that have reported effects related to the rubber hand illusion at similar locations (Press et al., 2008; Zeller et al., 2015; Rao and Kayser, 2017) and for comparison over parietal electrodes. See Materials and Methods for the effective number of data epochs for each condition.

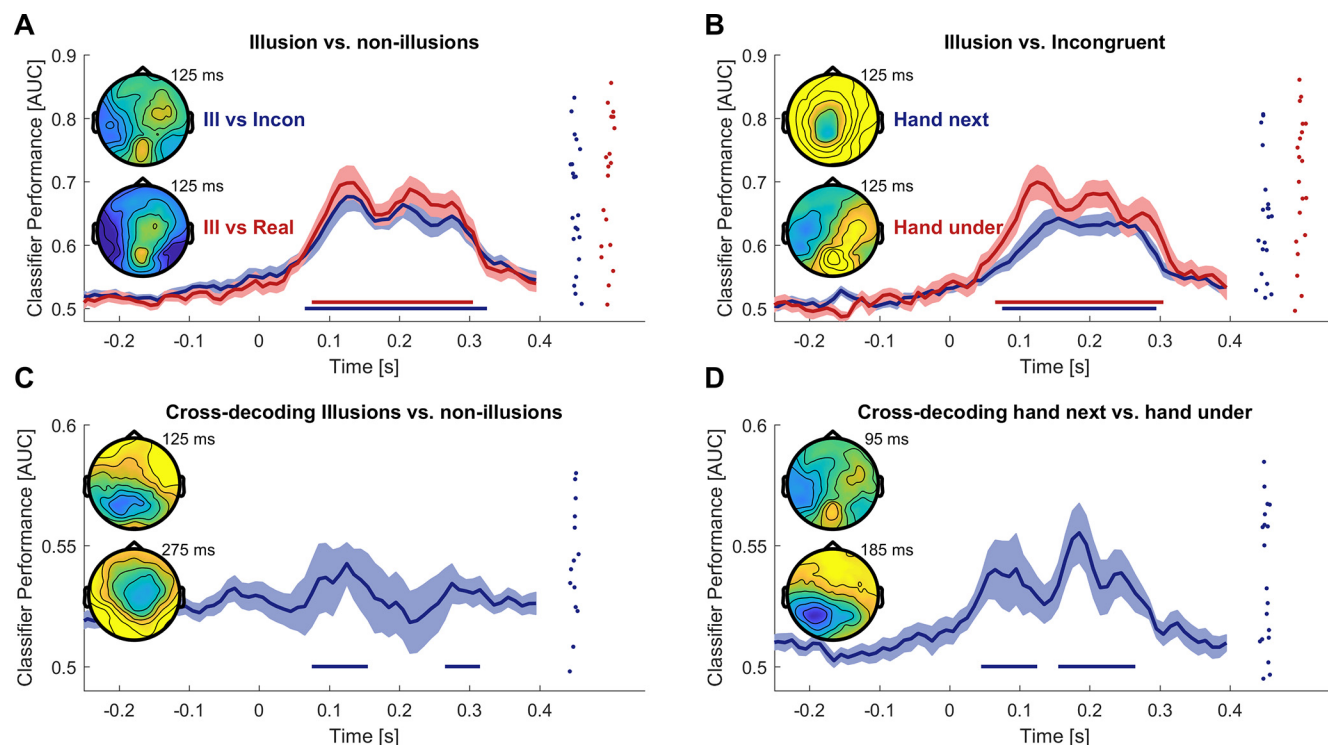


Figure 4. Classification analysis reveals long-lasting activations associated with the illusion. **A**, Contrasting evoked responses between Illusion and Incongruent conditions and between Illusion and the Real conditions using linear multivariate classification revealed significant classification performance for all comparisons. The time axis refers to the center of the time windows used for classification. Classifier performance was computed as the area under the receiver-operator characteristic (AUC). Thick curves indicate the mean and shaded areas indicate the SEM. Straight lines at the bottom indicate periods of significant performance (cluster-based permutation test corrected for multiple comparisons along time, at $p < 0.01$). Topographies indicated the group-averaged forward models (color scale -0.3 to 0.3), and dots indicate individual participant's classifier performance at the time points of maximal classifier performance (as indicated besides the topographies). **B**, Results for the classification between each individual Illusion condition and the respective Incongruent condition. **C**, Cross-classification analysis between Illusion versus Incongruent and Illusion versus Real conditions, probing for activations that reliably differentiate Illusion and non-Illusion epochs across experimental conditions. **D**, Cross-classification between each individual Illusion and its respective Incongruent condition, i.e., testing whether activity patterns differentiating Illusion and Incongruent “hand next” conditions also differentiate these for “hand under,” and vice versa. The individual data ($n = 22$) are from time points 125 ms (**A–C**) and 95 ms (**D**), respectively.

classification to confirm that the neurophysiological processes differentiating the Illusion and the Incongruent for the “hand next” conditions shared a similar spatial configuration compared with those differentiating these conditions during the “hand under” configuration: cross-classification was significant for most time points (between 0.045 and 0.125 s, $p = 0.002$, $AUC_{sum} = 0.32$; max $AUC = 0.54$ at 0.095 s; and between 0.155 and 0.265 s, $p < 0.001$, $AUC_{sum} = 0.48$; max $AUC = 0.56$ at 0.185 s; Fig. 4D). Together, these results suggest that the neurophysiological processes differentiating the Illusion from the non-Illusion conditions fall into two types: one that generalizes across non-Illusion conditions (Incongruent and Real), and one for which activity selectively differentiates the Illusion from just one of these control conditions.

Evoked responses differ within Illusion trials according to the subjective state

Comparisons between Illusion and control conditions are performed by comparing epochs from distinct

experimental trials provided at different times during the experiment. Hence these may differ not only in the subjective illusory state. In a separate analysis, we investigated a contrast to isolate correlates of the illusory state in which we aimed to render the comparison of illusion and non-illusion-related activity more specific; for this, we directly contrasted epochs characterized by the illusory state and those reflecting non-Illusion epochs within the same experimental Illusion trials (Ehrsson et al., 2004; Guterstam et al., 2019). We split the epochs from the Illusion trials into those before the illusion onset and those during illusory state based on participants' responses indicating the onset of the illusory state. A classification contrasting these epochs was significant ($n = 22$, cluster from 0.095 to 0.300 s, $p < 0.001$, $AUC_{sum} = 1.71$, max $AUC = 0.60$ at 0.155 s; Fig. 5A).

We then asked whether the activity patterns differentiating these pre-Illusion and Illusion epochs within the same experimental trials are similar to those differentiating the Illusion and Incongruent epochs between trials (compare Fig. 4A). To address this, we trained a classifier on

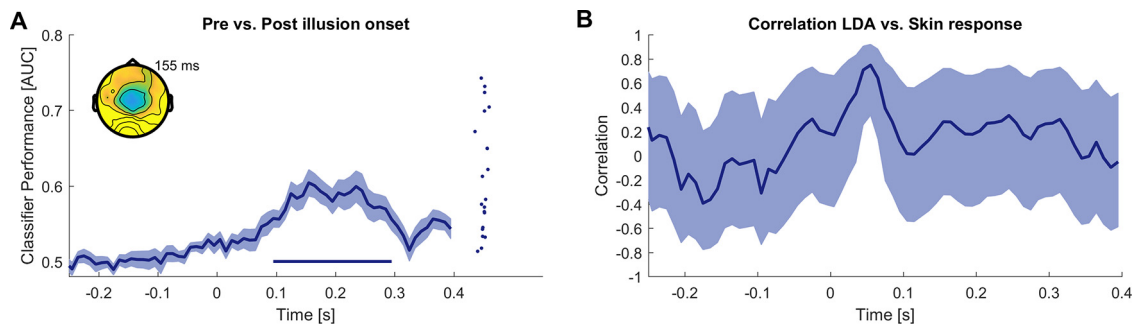


Figure 5. Within-trial illusion correlates and probing for an association with skin responses. **A**, Classification of EEG activity between epochs before the illusion onset and the epochs after the illusion onset within the Illusion trials. Thick curves indicate the mean and shaded areas indicate the standard errors of the mean. Straight lines at the bottom indicate periods of significant classification performance ($n=22$; cluster-based permutation test correcting for multiple comparisons along time, at $p < 0.01$). Scalp topographies show the classifier forward model and dots the individual classifier performance at the time point of maximal performance (color-scale -0.3 to 0.3). **B**, Results of a correlation analysis between the classification performance for Illusion versus Incongruent epochs and the difference in skin response between these conditions. The solid line indicates the group-level Pearson correlation, the shaded area the 95% confidence interval ($n=20$).

the pre-Illusion versus Illusion classification and tested whether this generalizes to the discrimination of Illusion versus Incongruent epochs: this cross-classification analysis did not yield any significance (cluster-based permutation tests, no clusters at the respective criteria; max AUC = 0.52 at 0.300 s).

Neurophysiological signatures of the illusion and skin responses

Given that the illusory state was associated with changes in EEG responses and with changes in skin conductance, we asked whether the respective effects were correlated across participants. To test this, we computed the correlation between the LDA classifier performance in discriminating Illusion and Incongruent epochs as a measure of the participant-wise illusion-effect in the EEG signal and the differences of skin responses in Illusion and the Incongruent conditions. We focused on the Illusion versus Incongruent comparison as for this specific comparison the skin responses had revealed a significant effect (compare Fig. 2). We found a no significant correlation ($n=20$ participants with usable skin responses; cluster-based permutation statistics; cluster from 0.035 to 0.065 s, trending $p=0.061$, sum = 2.61 peak value 0.75 and peak time 0.055 s).

Discussion

We investigated the neurophysiological correlates of the RHI using a multivariate (cross-)classification framework and asked whether and when evoked responses differentiate the illusory state reliably from multiple and different control conditions used to isolate correlates of the illusory state. Thereby the present study aimed to make both methodological and conceptual advances on our understanding of the neurophysiological signatures of body illusions such as the rubber hand, as discussed below. We found that EEG responses differed between Illusion and non-Illusion epochs starting at latencies of ~ 65 ms following stimulation onset and did so over a

prolonged time. Importantly, around two time points, 125 and 275 ms, the illusory state was reliably differentiated from multiple non-Illusion conditions by a common spatial pattern of evoked responses in each participant, pointing to neurophysiological processes possibly specifically associated with the illusory state.

Correlates of the illusory state in neurophysiological responses

A number of studies have aimed to understand the EEG-derived correlates of the RHI by investigating the responses evoked by the illusion-inducing stimuli (Press et al., 2008; Cardini et al., 2011; Zeller et al., 2015; Rao and Kayser, 2017; Guterstam et al., 2019). This approach rests on the idea that the neurophysiological signatures in the evoked response can reliably index the relevant neurophysiological processes differentiating the illusory state from suitable control conditions. However, these previous studies provide diverging results: while some report a modulation of evoked responses at early (55 ms) latencies (Otsuru et al., 2014; Zeller et al., 2015) others report effects around 140–200 ms (Press et al., 2008) or even later latencies such as between 300 and 450 ms (Rao and Kayser, 2017). Furthermore, while some studies suggest an enhanced evoked response during the illusory state (Press et al., 2008; Aspell et al., 2012), others rather point to a suppression (Zeller et al., 2015), or found no significant difference (Pyasik et al., 2021). Importantly, most studies effectively mapped group-level activations and made the implicit assumption that the neurophysiological sources differentiating Illusion and non-Illusion conditions have the same spatial (electrode-wise) configuration across participants, which may not be valid. In support of this notion, one study emphasized the distributed nature of the activity related to bodily illusions whereby distributed patterns may better reflect the illusory state rather than localized effects (Aspell et al., 2012). To shift the focus from group-level activations to a representational framework (Kriegeskorte et al., 2006; Hebart and Baker,

2018), we here exploited a multivariate classification approach. This allowed us to relax the assumption of a common spatial pattern of illusion-related evoked response across participants, providing a methodological shift from previous studies. Importantly, it also allowed us to directly test within each participant at which time point the relevant neurophysiological signatures generalize between conditions, such as the Incongruent and Real conditions, or horizontal and vertical arrangements of real and artificial hands. Along this conceptual level, our results show that evoked responses differ reliably between Illusion and non-Illusion epochs over prolonged periods (see Table 2 for an overview). This result effectively allows consolidating the previous work, as the present data support multiple of the previously reported illusion correlates.

The earliest differences between Illusion and non-Illusion epochs emerged around 65 ms from stimulus onset. This finding corroborates previous studies, which have pointed to such early illusion-correlates as possibly arising from somatosensory cortices (Zeller et al., 2015; Sakamoto and Ifuku, 2021). Still, these did not test whether these illusion-correlates generalize between control conditions. Addressing this, our cross-classification analysis suggests that at these latencies illusion-related neurophysiological signatures indeed generalize across distinct non-Illusion conditions.

Both the decoding and cross-classification performances peaked around 120–130 ms. The classifier forward models around these time points (compare Fig. 4) revealed a differential contribution of bilateral fronto-parietal sensors, as opposed to for example a lateralization of the relevant processes. A previous study using a full body illusion using a has attributed activations around these latencies to higher somatosensory and temporo-parietal regions involved in the integration of visual and tactile inputs about body position (Aspell et al., 2012).

Between 150 and 250 ms, the illusion-related processes generalized across hand positions (Illusion vs Incongruent contrast) but did not generalize to the Real condition, despite other activity patterns differentiating Illusion and Real conditions around the same time. Our interpretation is that activity during this time window reflects two kinds of processes: one that detects the spatiotemporal mismatch of the multisensory information between the visual and somatosensory inputs and gives rise to the difference between Illusion and Incongruent conditions. Another is sensitive to the embodied nature of the seen hand and whether the control object is posed in a realistic body position, giving rise to the difference between Illusion and Real conditions (Otsuru et al., 2014; Zeller et al., 2015).

Lastly, from ~265 to 315 ms, the illusory state could again be reliably differentiated from all control conditions by a common activity pattern in each participant. Previous work has attributed potential illusion-correlates at these latencies to higher parietal and frontal regions, which have been implied in the formation of the illusory state based on multiple lines of evidence (Ehrsson et al., 2004, 2005; Petkova et al., 2011; Blanke, 2012; Bekrater-Bodmann et al., 2014). Activity at these latencies may in principle reflect a number of

factors, such as spatial attention (Press et al., 2008; Rao and Kayser, 2017), bodily self-detection (Galigani et al., 2021) and high-level processes pertaining to multisensory causal inference (Samad et al., 2015; Ehrsson and Chancel, 2019; Fang et al., 2019), but again previous work has not shown that the neurophysiological representations differentiating the illusory state generalize across multiple control conditions. A parsimonious explanation may be that around these latencies parietal and premotor regions combine the available visual, tactile and proprioceptive signals with preexisting body representations to give rise to the illusory ownership feeling (Press et al., 2008; Lippert et al., 2013; Quinn et al., 2014).

The impact of methodological details on outcomes in studies on the RHI

A central issue with studies on the RHI or similar body illusions is that the experimental contrasts generated to isolate the neural correlates of the illusory state are not specific to just this subjective state. This is because the data obtained during the experimental conditions inducing the illusion and those during the respective control conditions differ along multiple dimensions. For example, the data obtained during the Incongruent control condition and the Illusion condition differ in that participants were experiencing the illusion only in the Illusion condition, but differ also in the orientation of the rubber hand (Kalckert and Ehrsson, 2012, 2014; Rao and Kayser, 2017). Similarly, the Illusion and the Real conditions differ in the nature of the viewed stimulated hand (Zeller et al., 2015, 2016; Rao and Kayser, 2017), and in some other studies the conditions inducing the illusion and serving as control differed in the temporal pattern of the applied sensory stimuli (Botvinick and Cohen, 1998; Bekrater-Bodmann et al., 2012; Riemer et al., 2015). As a result, it is difficult to associate the neurophysiological correlates of the illusory state obtained in any individual and pairwise statistical comparison with a unique aspect of this paradigm (Rao and Kayser, 2017). In a conceptual advance to overcome this problem, we combined multiple control conditions with multivariate cross-classification, which allowed us to directly probe which neurophysiological processes consistently differentiate the illusory state from more than one non-Illusion condition.

First, we employed two spatial configurations of participants and rubber hands for the Illusion conditions, by displacing the rubber and real hands either in the horizontal or vertical planes, while keeping their physical distance the same. Our results show that the hand under arrangement required less time to induce the illusion, in line with studies reporting stronger illusory precepts for the vertical set-up based on questionnaire scores (Bekrater-Bodmann et al., 2012) and with the general idea that distances in the horizontal and vertical plane are often judged differently (Loomis and Philbeck, 1999). Importantly, the neurophysiological signatures differentiating the Illusion and Incongruent conditions generalized across the precise spatial arrangement of hands at many time points, hence are independent of the spatial plane in which the illusion is induced. Second, we employed

both a rotated rubber hand and participant's own hand to generate control conditions not inducing the illusion (Zeller et al., 2015, 2016; Rao and Kayser, 2017). Neurophysiological signatures that reliably differentiate the illusory state from both control conditions, e.g., around 120–130 ms in our data, should hence be insensitive to the precise nature of the second hand in sight, or the precise position of the second hand relative to the own body. However, whether this renders the respective neurophysiological correlates specific to only the subjective illusory state still remains unclear, and future work could combine the multivariate approach with additional illusion configurations or other non-illusion control conditions.

In an attempt to overcome this conundrum around comparing distinct experimental configuration, we directly contrasted activity within the Illusion trials between epochs before and while participants were feeling the illusion. This contrast pertains only to the Illusion configuration and allows a comparison of EEG responses obtained during the very same sensory input. Still, one may argue that also this comparison is potentially confounded by additional factors, such as participant's task set (being ready to report the illusion onset before this, and having no task after the onset) or adaptation effects because of the repetitive stimulation of the somatosensory system over prolonged time (McLaughlin and Kelly, 1993). The cross-decoding results suggest that the neurophysiological processes differentiating the Illusion condition from both Incongruent and Real conditions may not allow differentiating the epochs before and following the onset of the illusory state in the Illusion trials, possibly for the above-mentioned reasons. This leaves it for future studies to probe whether there are indeed neurophysiological signatures of the rubber hand illusion that are genuinely specific to the illusory state and not confounded by additional factors.

The present study was based on a multivariate classification framework. This allowed us to relax the possibly invalid assumption made in previous studies that illusion-related activations have the same spatial configuration across participants. While this allowed us to derive time points at which brain activity possibly characterizes the illusory state, it makes it difficult to associate the underlying neurophysiological processes with specific brain regions. Future studies, for example relying on combined EEG-fMRI recordings, may capitalize on the present experimental and analytical approach to more precisely determine the brain regions correlating with or giving rise to the differences between Illusion and non-Illusion conditions. Such studies may also be able to determine whether processes differentiating epochs before and subsequent the illusion are indeed genuinely different from those differentiating, for example, Illusion from the Incongruent or the Real condition.

Changes in skin conductance and body illusions

Bodily signals such as changes in skin conductance are frequently studied in the context of body illusions, yet their suitability as markers of the illusory state remain

debated (Holle et al., 2011; Kammers et al., 2011; Holmes et al., 2012; Suzuki et al., 2013; Riemer et al., 2015; Crucianelli et al., 2018; Horváth et al., 2020). Often, a threat is applied to the embodied rubber hand, which induces changes in skin conductance compared with control conditions (Armell and Ramachandran, 2003; Ehrsson et al., 2007), although some studies also focused on skin conductance during the entire experimental trial (D'Alonzo et al., 2020). We here focused on the moments at which the illusory state emerged and asked whether this emergence is characterized by concomitant changes in skin conductance. Our data support a change in bodily state prior participants' actual overt response of reporting the illusion, possibly because changes in arousal precede the subjective sensation of ownership. This finding seems in line with the general idea that changes in arousal are associated or can precede cognitive processes (Bechara et al., 1997; Critchley et al., 2000; Williams et al., 2000; Critchley, 2002; Dawson et al., 2011). The associated skin response was significant in comparison to the Incongruent but not when compared with the Real condition, reflecting a stronger skin response relative to the embodiment of the stimulated rubber hand, which does not happen in contrast to the stimulation of a real embodied hand. Furthermore, the skin responses were not correlated with the electrophysiological signatures, leaving it unclear whether and to what degree bodily and neurophysiological markers of the illusion reflect the same underlying processes (Holle et al., 2011; Kammers et al., 2011; Holmes et al., 2012; Riemer et al., 2015; Horváth et al., 2020).

In conclusion, by probing the correlates of the rubber hand illusion using a multivariate (cross-)classification framework we make a methodological step toward understanding those neurophysiological signatures of body illusions that are independent of the precise experimental configuration or statistical contrasts used to isolate these. Consolidating previous work, our results suggest that evoked responses around 125 and 275 ms may be interesting candidate time points for future studies, though they also highlight the interpretational difficulties when interpreting the correlates of subjective states such as body illusions.

References

- Armell KC, Ramachandran VS (2003) Projecting sensations to external objects: evidence from skin conductance response. *Proc Biol Sci* 270:1499–1506.
- Aspell JE, Palluel E, Blanke O (2012) Early and late activity in somatosensory cortex reflects changes in bodily self-consciousness: an evoked potential study. *Neuroscience* 216:110–122.
- Bechara A, Damasio H, Tranel D, Damasio AR (1997) Deciding advantageously before knowing the advantageous strategy. *Science* 275:1293–1295.
- Bekrater-Bodmann R, Foell J, Diers M, Flor H (2012) The perceptual and neuronal stability of the rubber hand illusion across contexts and over time. *Brain Res* 1452:130–139.
- Bekrater-Bodmann R, Foell J, Diers M, Kamping S, Rance M, Kirsch P, Trojan J, Fuchs X, Bach F, Çakmak HK, Maaß H, Flor H (2014) The importance of synchrony and temporal order of visual and tactile input for illusory limb ownership experiences – an fMRI study applying virtual reality. *PLoS One* 9:e87013.

- Bertamini M, O'Sullivan N (2014) The use of realistic and mechanical hands in the rubber hand illusion, and the relationship to hemispheric differences. *Conscious Cogn* 27:89–99.
- Blanke O (2012) Multisensory brain mechanisms of bodily self-consciousness. *Nat Rev Neurosci* 13:556–571.
- Blankertz B, Lemm S, Treder M, Haufe S, Müller K-R (2011) Single-trial analysis and classification of ERP components—a tutorial. *Neuroimage* 56:814–825.
- Botvinick M, Cohen J (1998) Rubber hands ‘feel’ touch that eyes see. *Nature* 391:756–756.
- Boucsein W, Fowles DC, Grimnes S, Ben-Shakhar G, Roth WT, Dawson ME, Filion DL; Society for Psychophysiological Research Ad Hoc Committee on Electrodermal Measures (2012) Publication recommendations for electrodermal measurements. *Psychophysiology* 49:1017–1034.
- Bröhl F, Kayser C (2021) Delta/theta band EEG differentially tracks low and high frequency speech-derived envelopes. *Neuroimage* 233:117958.
- Brozzoli C, Gentile G, Ehrsson HH (2012) That’s near my hand! Parietal and premotor coding of hand-centered space contributes to localization and self-attribution of the hand. *J Neurosci* 32:14573–14582.
- Campos Viola F, Thorne J, Edmonds B, Schneider T, Eichele T, Debener S (2009) Semi-automatic identification of independent components representing EEG artifact. *Clin Neurophysiol* 120:868–877.
- Cardini F, Longo MR, Haggard P (2011) Vision of the body modulates somatosensory intracortical inhibition. *Cereb Cortex* 21:2014–2022.
- Cardini F, Longo MR, Driver J, Haggard P (2012) Rapid enhancement of touch from non-informative vision of the hand. *Neuropsychologia* 50:1954–1960.
- Cichy RM, Teng S (2017) Resolving the neural dynamics of visual and auditory scene processing in the human brain: a methodological approach. *Philos Trans R Soc Lond B Biol Sci* 372:20160108.
- Cichy RM, Pantazis D, Oliva A (2014) Resolving human object recognition in space and time. *Nat Neurosci* 17:455–462.
- Costantini M, Robinson J, Migliorati D, Donno B, Ferri F, Northoff G (2016) Temporal limits on rubber hand illusion reflect individuals’ temporal resolution in multisensory perception. *Cognition* 157:39–48.
- Critchley HD (2002) Electrodermal responses: what happens in the brain. *Neuroscientist* 8:132–142.
- Critchley HD, Elliott R, Mathias CJ, Dolan RJ (2000) Neural activity relating to generation and representation of galvanic skin conductance responses: a functional magnetic resonance imaging study. *J Neurosci* 20:3033–3040.
- Crucianelli L, Krahe C, Jenkinson PM, Fotopoulou AK (2018) Interoceptive ingredients of body ownership: affective touch and cardiac awareness in the rubber hand illusion. *Cortex* 104:180–192.
- D’Alonzo M, Mioli A, Formica D, Di Pino G (2020) Modulation of body representation impacts on efferent autonomic activity. *J Cogn Neurosci* 32:1104–1116.
- Dawson ME, Schell AM, Courtney CG (2011) The skin conductance response, anticipation, and decision-making. *J Neurosci Psychol Econ* 4:111–116.
- Ehrsson HH, Chancel M (2019) Premotor cortex implements causal inference in multisensory own-body perception. *Proc Natl Acad Sci USA* 116:19771–19773.
- Ehrsson HH, Spence C, Passingham RE (2004) That’s my hand! Activity in premotor cortex reflects feeling of ownership of a limb. *Science* 305:875–877.
- Ehrsson HH, Holmes NP, Passingham RE (2005) Touching a rubber hand: feeling of body ownership is associated with activity in multisensory brain areas. *J Neurosci* 25:10564–10573.
- Ehrsson HH, Wiech K, Weiskopf N, Dolan RJ, Passingham RE (2007) Threatening a rubber hand that you feel is yours elicits a cortical anxiety response. *Proc Natl Acad Sci USA* 104:9828–9833.
- Eichert N, Robinson EC, Bryant KL, Jbabdi S, Jenkinson M, Li L, Krug K, Watkins KE, Mars RB (2020) Cross-species cortical alignment identifies different types of anatomical reorganization in the primate temporal lobe. *Elife* 9:e53232.
- Evans N, Blanke O (2013) Shared electrophysiology mechanisms of body ownership and motor imagery. *Neuroimage* 64:216–228.
- Fang W, Li J, Qi G, Li S, Sigman M, Wang L (2019) Statistical inference of body representation in the macaque brain. *Proc Natl Acad Sci USA* 116:20151–20157.
- Fuchs X, Riemer M, Diers M, Flor H, Trojan J (2016) Perceptual drifts of real and artificial limbs in the rubber hand illusion. *Sci Rep* 6:24362.
- Galigani M, Ronga I, Fossataro C, Bruno V, Castellani N, Rossi Sebastiano A, Forster B, Garbarini F (2021) Like the back of my hand: visual ERPs reveal a specific change detection mechanism for the bodily self. *Cortex* 134:239–252.
- Gentile G, Guterstam A, Brozzoli C, Ehrsson HH (2013) Disintegration of multisensory signals from the real hand reduces default limb self-attribution: an fMRI study. *J Neurosci* 33:13350–13366.
- Grabot L, Kayser C (2020) Alpha activity reflects the magnitude of an individual bias in human perception. *J Neurosci* 40:3443–3454.
- Grootswagers T, Cichy RM, Carlson TA (2018) Finding decodable information that can be read out in behaviour. *Neuroimage* 179:252–262.
- Grootswagers T, Wardle SG, Carlson TA (2017) Decoding dynamic brain patterns from evoked responses: a tutorial on multivariate pattern analysis applied to time series neuroimaging data. *J Cogn Neurosci* 29:677–697.
- Guggenmos M, Sterzer P, Cichy RM (2018) Multivariate pattern analysis for MEG: a comparison of dissimilarity measures. *Neuroimage* 173:434–447.
- Guterstam A, Gentile G, Ehrsson HH (2013) The invisible hand illusion: multisensory integration leads to the embodiment of a discrete volume of empty space. *J Cogn Neurosci* 25:1078–1099.
- Guterstam A, Björnsdotter M, Gentile G, Ehrsson HH (2015) Posterior cingulate cortex integrates the senses of self-location and body ownership. *Curr Biol* 25:1416–1425.
- Guterstam A, Collins KL, Cronin JA, Zeberg H, Darvas F, Weaver KE, Ojemann JG, Ehrsson HH (2019) Direct electrophysiological correlates of body ownership in human cerebral cortex. *Cereb Cortex* 29:1328–1341.
- Hebart MN, Baker CI (2018) Deconstructing multivariate decoding for the study of brain function. *Neuroimage* 180:4–18.
- Hipp JF, Siegel M (2013) Dissociating neuronal gamma-band activity from cranial and ocular muscle activity in EEG. *Front Hum Neurosci* 7:338.
- Holle H, McLatchie N, Maurer S, Ward J (2011) Proprioceptive drift without illusions of ownership for rotated hands in the “rubber hand illusion” paradigm. *Cogn Neurosci* 2:171–178.
- Holmes NP, Makin TR, Cadieux M, Williams C, Naish KR, Spence C, Shore DI (2012) Hand ownership and hand position in the rubber hand illusion are uncorrelated. *Seeing Perceiving* 25:52.
- Horváth Á, Ferentzi E, Bogdány T, Szolcsányi T, Witthöft M, Köteles F (2020) Proprioception but not cardiac interoception is related to the rubber hand illusion. *Cortex* 132:361–373.
- Kalckert A, Ehrsson HH (2012) Moving a rubber hand that feels like your own: a dissociation of ownership and agency. *Front Hum Neurosci* 6:40.
- Kalckert A, Ehrsson HH (2014) The moving rubber hand illusion revisited: comparing movements and visuotactile stimulation to induce illusory ownership. *Conscious Cogn* 26:117–132.
- Kammers MPM, Rose K, Haggard P (2011) Feeling numb: temperature, but not thermal pain, modulates feeling of body ownership. *Neuropsychologia* 49:1316–1321.
- Kaplan JT, Man K, Greening SG (2015) Multivariate cross-classification: applying machine learning techniques to characterize abstraction in neural representations. *Front Hum Neurosci* 9:151.
- Kayser SJ, Kayser C (2020) Shared physiological correlates of multisensory and expectation-based facilitation. *eNeuro* 7:ENEURO.0435-19.2019.

- Keitel A, Gross J, Kayser C (2020) Shared and modality-specific brain regions that mediate auditory and visual word comprehension. *Elife* 9:e56972.
- Kerby DS (2014) The simple difference formula: an approach to teaching nonparametric correlation. *Compr Psychol* 3:11.IT.3.1.
- Kriegeskorte N, Goebel R, Bandettini P (2006) Information-based functional brain mapping. *Proc Natl Acad Sci USA* 103:3863–3868.
- Li M, Wang D, Ren J, Langs G, Stoecklein S, Brennan BP, Lu J, Chen H, Liu H (2019) Performing group-level functional image analyses based on homologous functional regions mapped in individuals. *PLoS Biol* 17:e2007032.
- Limanowski J, Blankenburg F (2016) Integration of visual and proprioceptive limb position information in human posterior parietal, premotor, and extrastriate cortex. *J Neurosci* 36:2582–2589.
- Lippert MT, Takagaki K, Kayser C, Ohl FW (2013) Asymmetric multi-sensory interactions of visual and somatosensory responses in a region of the rat parietal cortex. *PLoS One* 8:e63631.
- Lloyd DM (2007) Spatial limits on referred touch to an alien limb may reflect boundaries of visuo-tactile peripersonal space surrounding the hand. *Brain Cogn* 64:104–109.
- Longo MR, Haggard P (2012) What is it like to have a body? *Curr Dir Psychol Sci* 21:140–145.
- Loomis JM, Philbeck JW (1999) Is the anisotropy of perceived 3-D shape invariant across scale? *Percept Psychophys* 61:397–402.
- Maris E, Oostenveld R (2007) Nonparametric statistical testing of EEG- and MEG-data. *J Neurosci Methods* 164:177–190.
- McLaughlin DF, Kelly EF (1993) Evoked potentials as indices of adaptation in the somatosensory system in humans: a review and prospectus. *Brain Res Brain Res Rev* 18:151–206.
- Nichols TE, Holmes AP (2002) Nonparametric permutation tests for functional neuroimaging: a primer with examples. *Hum Brain Mapp* 15:1–25.
- O’Beirne GA, Patuzzi RB (1999) Basic properties of the sound-evoked post-auricular muscle response (PAMR). *Hear Res* 138:115–132.
- Oostenveld R, Fries P, Maris E, Schoffelen JM (2011) FieldTrip: open source software for advanced analysis of MEG, EEG, and invasive electrophysiological data. *Comput Intell Neurosci* 2011:e156869.
- Otsuru N, Hashizume A, Nakamura D, Endo Y, Inui K, Kakigi R, Yuge L (2014) Sensory incongruence leading to hand disownership modulates somatosensory cortical processing. *Cortex* 58:1–8.
- Park H, Kayser C (2019) Shared neural underpinnings of multisensory integration and trial-by-trial perceptual recalibration in humans. *Elife* 8:e47001.
- Park H, Kayser C (2021) The neurophysiological basis of the trial-wise and cumulative ventriloquism aftereffects. *J Neurosci* 41:1068–1079.
- Parra LC, Spence CD, Gerson AD, Sajda P (2005) Recipes for the linear analysis of EEG. *Neuroimage* 28:326–341.
- Pavani F, Spence C, Driver J (2000) Visual capture of touch: out-of-the-body experiences with rubber gloves. *Psychol Sci* 11:353–359.
- Peled A, Pressman A, Geva AB, Modai I (2003) Somatosensory evoked potentials during a rubber-hand illusion in schizophrenia. *Schizophr Res* 64:157–163.
- Petkova VI, Björnsdotter M, Gentile G, Jonsson T, Li T-Q, Ehrsson HH (2011) From part- to whole-body ownership in the multisensory brain. *Curr Biol* 21:1118–1122.
- Press C, Heyes C, Haggard P, Eimer M (2008) Visuotactile learning and body representation: an ERP study with rubber hands and rubber objects. *J Cogn Neurosci* 20:312–323.
- Preston C (2013) The role of distance from the body and distance from the real hand in ownership and disownership during the rubber hand illusion. *Acta Psychol (Amst)* 142:177–183.
- Pyasik M, Ronga I, Burin D, Salatino A, Sarasso P, Garbarini F, Ricci R, Pia L (2021) I’m a believer: illusory self-generated touch elicits sensory attenuation and somatosensory evoked potentials similar to the real self-touch. *Neuroimage* 229:117727.
- Quinn BT, Carlson C, Doyle W, Cash SS, Devinsky O, Spence C, Halgren E, Thesen T (2014) Intracranial cortical responses during visual-tactile integration in humans. *J Neurosci* 34:171–181.
- Rao IS, Kayser C (2017) Neurophysiological correlates of the rubber hand illusion in late evoked and alpha/beta band activity. *Front Hum Neurosci* 11:377.
- Reader AT, Trifonova VS, Ehrsson HH (2021) The relationship between referral of touch and the feeling of ownership in the rubber hand illusion. *Front Psychol* 12:629590.
- Riemer M, Bublatzky F, Trojan J, Alpers GW (2015) Defensive activation during the rubber hand illusion: ownership versus proprioceptive drift. *Biol Psychol* 109:86–92.
- Riemer M, Trojan J, Beauchamp M, Fuchs X (2019) The rubber hand universe: on the impact of methodological differences in the rubber hand illusion. *Neurosci Biobehav Rev* 104:268–280.
- Rohde M, Di Luca M, Ernst MO (2011) The rubber hand illusion: feeling of ownership and proprioceptive drift do not go hand in hand. *PLoS One* 6:e21659.
- Sakamoto M, Ifuku H (2021) Attenuation of sensory processing in the primary somatosensory cortex during rubber hand illusion. *Sci Rep* 11:7329.
- Samad M, Chung AJ, Shams L (2015) Perception of body ownership is driven by Bayesian sensory inference. *PLoS One* 10:e0117178.
- Shimada S, Fukuda K, Hiraki K (2009) Rubber Hand illusion under delayed visual feedback. *PLoS One* 4:e6185.
- Sjouwerman R, Lonsdorf TB (2019) Latency of skin conductance responses across stimulus modalities. *Psychophysiology* 56:e13307.
- Suzuki K, Garfinkel SN, Critchley HD, Seth AK (2013) Multisensory integration across exteroceptive and interoceptive domains modulates self-experience in the rubber-hand illusion. *Neuropsychologia* 51:2909–2917.
- Tsakiris M, Haggard P (2005) The rubber hand illusion revisited: visuotactile integration and self-attribution. *J Exp Psychol Hum Percept Perform* 31:80–91.
- Valenzuela Moguillansky C, O’Regan JK, Petitmengin C (2013) Exploring the subjective experience of the “rubber hand” illusion. *Front Hum Neurosci* 7:659.
- Van Horn JD, Grafton ST, Miller MB (2008) Individual variability in brain activity: a nuisance or an opportunity? *Brain Imaging Behav* 2:327–334.
- Williams LM, Brammer MJ, Skerrett D, Lagopoulos J, Rennie C, Kozek K, Olivieri G, Peduto T, Gordon E (2000) The neural correlates of orienting: an integration of fMRI and skin conductance orienting. *Neuroreport* 11:3011–3015.
- Zeller D, Litvak V, Friston KJ, Classen J (2015) Sensory processing and the rubber hand illusion—an evoked potentials study. *J Cogn Neurosci* 27:573–582.
- Zeller D, Friston KJ, Classen J (2016) Dynamic causal modeling of touch-evoked potentials in the rubber hand illusion. *Neuroimage* 138:266–273.